Porosity evaluation of PoSi wafer using a nondestructive ultrasonic technic

Julien Bustillo, Jérôme Fortineau, Marie Capelle, François Vander Meulen, Lionel Haumesser, Gael Gautier, Marc Lethiecq

Porosity evaluation of PoSi wafer using a nondestructive ultrasonic technic

J. Bustillo[a], J. Fortineau[a], M. Capelle[b], F. Vander Meulen[a], L. Haumesser[a], G. Gautier[b] and M. Lethiecq[a]

[a]Université François Rabelais de Tours, GREMAN, ENIVL, Rue de la Chocolaterie BP 3410, 41034 Blois, France

[b]Université François Rabelais de Tours, GREMAN, 16 rue Pierre et Marie Curie, BP 7155, 37071 Tours Cedex 2, France

julien.bustillo@univ-tours.fr

The manufacturing processes of porous silicon (PoSi) now allow samples with variable depths and variable degrees of porosity to be obtained. However, thickness and porosity measurement methods of PoSi are currently destructive. Therefore in this study a nondestructive ultrasonic method is developed. For this, an immersion insertion-substitution technique has been used. Samples with different porosity depth and porosity rates are studied. The thickness of the wafer (650 μm) and high sound speed in pure silicon (8450 m/s) require transducers with high central frequencies (from 15 to 50 MHz). The acoustic parameters of the wafer, such as velocity and attenuation are measured.

1 Introduction

Electrochemical etching of silicon (Si) in HydroFluoric acid (HF) based solutions is nowadays a very well-known process and numerous reports have been made on the porous silicon (PoSi) growth mechanisms [1, 2]. In the wide range of morphologies that can be produced, one can distinguish microporous Si, a sponge-like structure of 1 to 5 nm crystallites, macroporous Si, mostly tubular pores with diameters up to 50 nm and, an intermediate category, the mesoporous Si with sizes between 5 and 50 nm [3]. This material has found many applications in microelectronics. One can point out for example, the use of mesoporous Si as an isolating substrate for RF applications [4, 5] or the application of the high specific surface of PoSi in sensors [6]. Mesoporous silicon is mainly produced from highly doped silicon (more than 1018 cm-3). When such a material is immersed into an HF solution, the interface reacts as a Schottky contact. Then, a very thin space charge region (SCR) is localized at the electrolyte\Si interface and acts as a passivation region against silicon dissolution on the pore walls. The hole diffusion, at the origin of the reaction, is then mainly ensured by a tunneling mechanism located at the pore tip [7]. The observed morphologies are consequently most of the time very anisotropic (Figure 1). Moreover, in high current density regimes, the pore growth direction is governed by the crystallography [8]. This particular morphology leads to very specific properties. Moreover, in many applications, one needs to obtain thick layers with a constant porosity or constant pore diameters in short times.

The measurement of the PoSi parameters, such as thickness or porosity, is currently destructive and cannot be used to monitor the fabrication process. Using the strong relationship between the mechanical properties of a medium and the properties of an elastic wave travelling through it, ultrasonic non-destructive testing can be a good way to measure these parameters [9]. Using a non-contact method is also essential for microelectronics, due to the contamination risk.

2 Materials

2.1 Fabrication of the PoSi layers

The PoSi layers were formed by the anodization in HF based solutions of highly doped p-type Si (10-50 mΩ.cm) <111> samples with thicknesses varying between 650 and 700 μm. This material is known to produce mesoporous silicon with pore diameters between 10 and 100 nm [7]. The electrochemical etching was performed in a double tank electrochemical cell developed by AMMT. The HF concentration is 30% and the surfactant used is acetic acid with volume ratios HF (50%): Acetic acid: H_2O of 4.6 : 2.1 : 1.5. The anodization was performed in a galvanostatic mode. A current density of 28 mA/cm^2 was fixed to obtain an average porosity of 50%. Then, the duration determined the total thickness of the porous layers. In our case, a duration of 87, 174 and 270 minutes lead to 100, 200 and 300 μm respectively. The average technological dispersion is in the range of 5 to 10%.

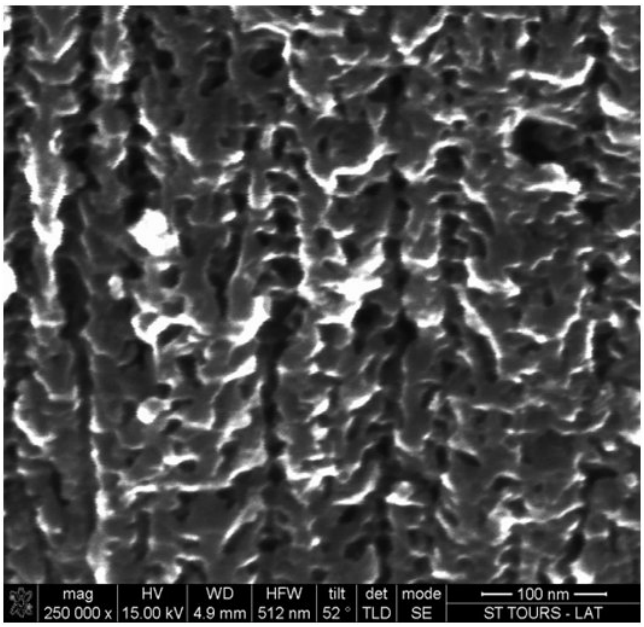

Figure 1: SEM observations of a n-type mesoporous sample from previous work. It was etched in a HF/H_2O (30%) electrolyte without any additive, using a current density of 43.6 mA/cm^2 during 30 minutes. The pore diameters are between 10 and 20 nm.

2.2 Materials specification

The samples used for this study are square-shaped crystalline silicon wafers on which a circular shaped PoSi layer with a one inch (2.54 cm) diameter is etched. This diameter is higher than that of the active surface of the piezoelectric transducer to ensure that all the ultrasonic signal passes through the porous medium.

In order to guarantee the precision of the final results, the wafer thickness is checked using a digital micrometer and values are summarised in Table 1. The physical parameters of the crystalline silicon and water used for this study are noted in Table 2 [10]. The speed of sound in water is strongly dependant on temperature [11]. In our study, the temperature of the water is kept constant at 20°C and monitored using a thermometer.

Table 1: Sample geometrical characteristics.

Sample number	Wafer thickness	Expected PoSi thickness
1	674±1 μm	0 μm
2	675±1 μm	300±30 μm
3	683±1 μm	200±20 μm
4	680±1 μm	100±10 μm

Table 2: Material properties at 20°C.

	Silicon	Water
Density ρ	2329 kg/m^3	1000 kg/m^3
Speed of sound C	8433 m/s	1480 m/s

3 Experimental approach

3.1 Insertion-substitution method

Figure 2 presents the insertion/substitution principle used to determine the velocity and the attenuation of the acoustic waves propagating in the samples based on broad-band transmission [12].

First, a measurement of the signal transmitted through the reference medium (water) is performed (top of Figure 2). The sample is then inserted between the two transducers (bottom of Figure 2).

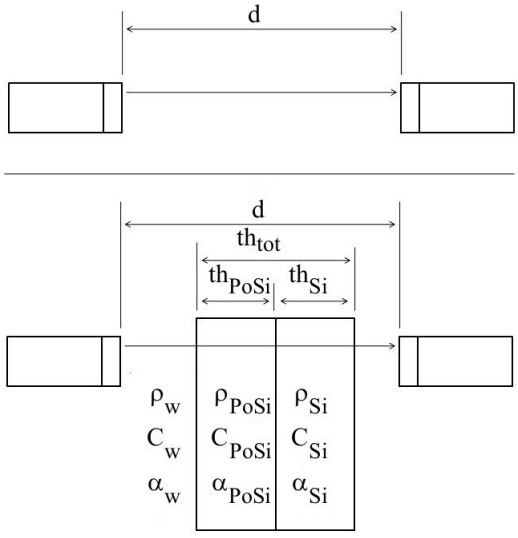

Figure 2: Insertion/substitution principle.

The signals which are measured at the receiver are respectively A_s for the signal which passes through the sample and A_{ref} for the reference signal (respectively Eq. 1 and Eq. 2).

$$A_s = A_0 \cdot T_{w-PoSi} \cdot T_{PoSI-Si} \cdot T_{Si-w} \cdot e^{-\alpha_w \cdot (d-th_{Si})} \cdot e^{-\alpha_{PoSi} \cdot th_{PoSi}} \cdot e^{-\alpha_{Si} \cdot (th_{Si}-th_{PoSi})} \quad (1)$$

$$A_ref = A_0 \cdot e^{-\alpha_w \cdot d} \quad (2)$$

where T_{ij} is the transmission coefficient between the medium i to the medium j, defined in Eq. 3, and α_i is the attenuation coefficient of medium i.

A_0 is the initial amplitude of the ultrasonic pulse.

$$T_{ij} = \frac{2 \cdot Z_j}{Z_i + Z_j} \quad (3)$$

where $Z_i = \rho_i \cdot C_i$ is the acoustic impedance of medium i. The density of the porous silicon can be defined as shown in Eq. 4 where p is the porosity rate.

$$\rho_{PoSi} = p \cdot \rho_w + (1-p) \cdot \rho_{Si} \quad (4)$$

The variation of the time of flight of the ultrasonic pulse through the sample allows the effective speed of sound C_{eff} in the sample to be calculated (Eq. 5)

$$C_{eff} = \frac{C_w \cdot th_{tot}}{\Delta t \cdot C_w + th_{tot}} \quad (5)$$

$$\Delta t = t_s - t_{ref} \quad (6)$$

The times of flight are named respectively t_s and t_{ref} for the signal through the sample and for the reference.

The ratio $\frac{A_s}{A_{ref}}$ given in Eq. 7 depends strongly on the sample properties, such as thickness and attenuation. This ratio is independent of the transducer characteristics thanks to the insertion-substitution method.

$$\frac{A_s}{A_{ref}} = T_{w-PoSi} \cdot T_{PoSI-Si} \cdot T_{Si-w}\, e^{\alpha_w \cdot th_{Si}} \cdot e^{-\alpha_{PoSi} \cdot th_{PoSi}} \cdot e^{-\alpha_{Si} \cdot (th_{Si}-th_{PoSi})} \quad (7)$$

The literature gives low attenuation coefficients for water [13] and crystalline Silicon [14]. The small thickness of the wafer allows these effects to be neglected in Eq. 7: the only attenuation is that of the PoSi layer, so its coefficient is easy to calculate using Eq. 8.

$$\alpha_{PoSi} \approx -\frac{\ln\left(\frac{A_s}{A_{ref} \cdot T_{w-PoSi} \cdot T_{PoSI-Si} \cdot T_{Si-w}}\right)}{th_{PoSi}} \quad (8)$$

3.2 Experimental setup

The experimental setup allowing the velocity and attenuation of the ultrasonic wave to be measured is shown in Figure 3. Two transducers with a centre frequency of 20 MHz (Figure 4) are set facing each other in water. The emission transducer is a 0.25 inch (8 mm) diameter Technisonic planar immersion transducer. It is driven by a pulse delivered by an Agilent 33250A waveform generator. After propagation through the sample, the wave is received by another similar transducer. The received signal is recorded by a LeCroy waveRunner 64XI digital oscilloscope at a sampling rate of 5GS/s. In order to increase the signal to noise ratio, a 1024 sweep averaging is performed.

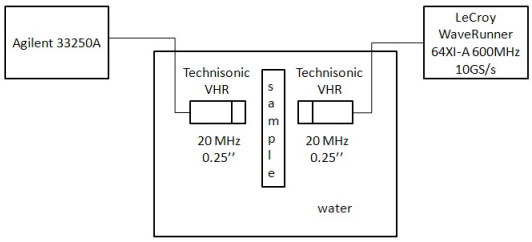

Figure 3: Apparatus for the insertion/substitution method.

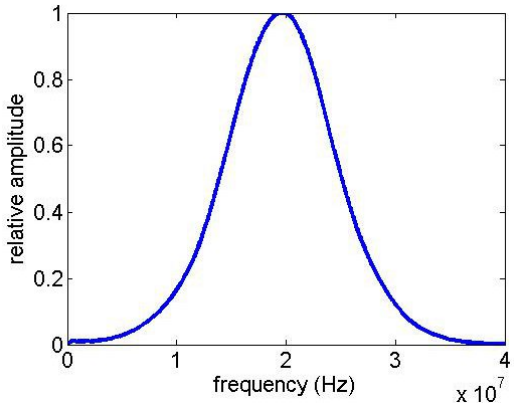

Figure 4: Spectrum of the reference signal.

The data processing is performed using Matlab following the diagram shown in Figure 5. The amplitude and the time delay are measured on the Hilbert transform of the signal, which allows the measurement precision to be enhanced.

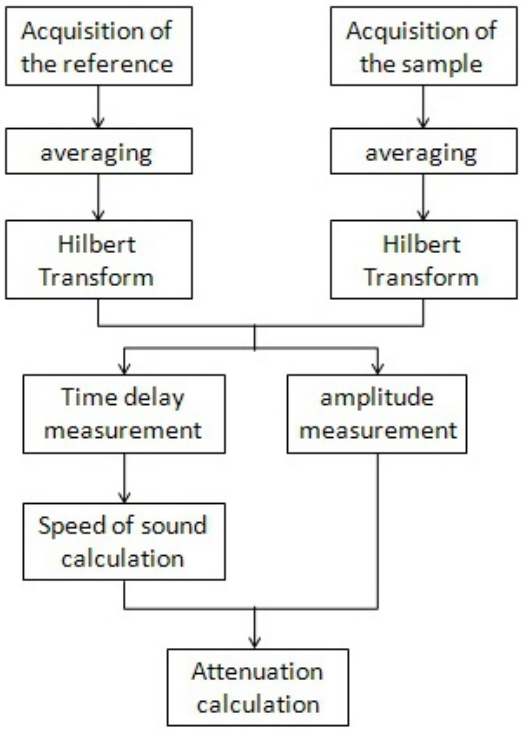

Figure 5: Signal processing diagram.

4 Results and discussion

4.1 Time Domain measurement

The measurement of the different parameters of the signal, such as time of flight and signal amplitude, is carried out on the Hilbert transform (Figure 6).

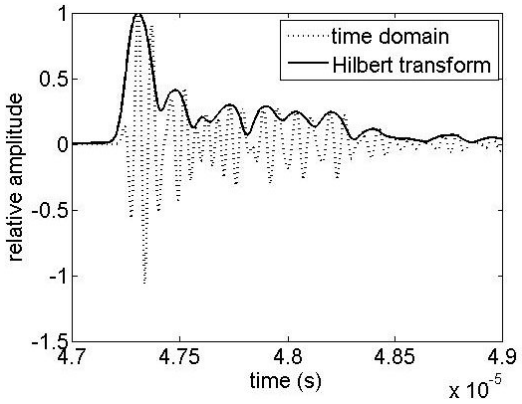

Figure 6: Time domain signal of the wave transmitted through sample 1 and its Hilbert transform.

The signal acquired after the propagation through the sample has a complex ring-down due to overlapping of return trips in the sample thickness (Figure 6). The determination of attenuation and velocity of the ultrasonic wave is performed in time domain since overlapping prohibits frequency-domain analysis. The values obtained will be averages in the transducer bandwidth.

4.2 Speed of sound in PoSi

This variation is measured using a threshold (Figure 7). The chosen threshold level is 10% of the maximum of the signal envelope because the signal envelopes in time domain all have very similar aspects.

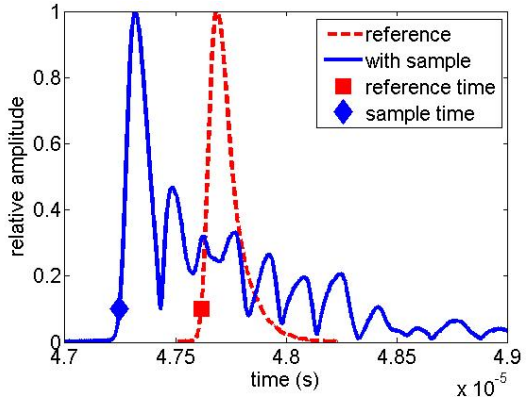

Figure 7: Hilbert transform of the reference signal and the signal through sample 1.

The measured values for the delay time δt and the calculated effective speed of sound in the sample are shown in table 3.

Table 3: Speed of sound measurements.

PoSi thickness	Delay time	Effective speed of sound
0 μm	376±1 ns	8430±100 m/s
100 μm	372±1 ns	7740±100 m/s
200 μm	363±1 ns	6960±100 m/s
300 μm	349±1 ns	6300±100 m/s

Figure 8 presents the variation of the effective speed of sound in the sample as a function of the expected PoSi layer thickness. This variation is monotonous. The effective speed of sound in the sample when the silicon is in this crystalline form (Eq. 10) is close to the values from literature (Table 2).

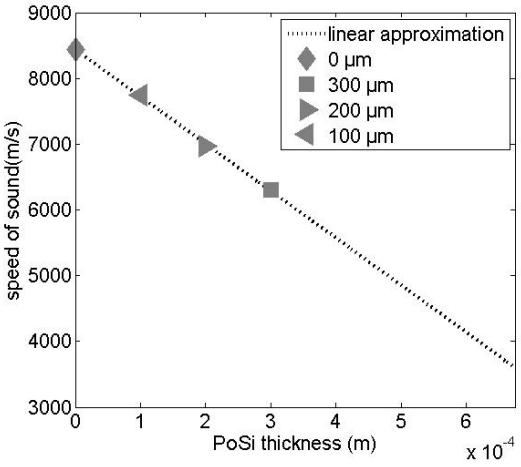

Figure 8: Effective speed of sound in function of the expected PoSi layer thickness.

The experimental values are close to the linear approximation (Eq. 9) allowing the calculation of the speed of sound in the PoSi layer using the Eq 10.

$$C_{eff} = x \cdot C_{PoSi} + (1 - x) \cdot C_{Si} \tag{9}$$

$$C_{PoSi} = \frac{C_{eff} - (1 - x) \cdot C_{Si}}{x},\ 0 < x \leq 1 \tag{10}$$

where:

$$x = \frac{th_{PoSi}}{th_{tot}} \tag{11}$$

The limits of the effective linear approximation are given in Eq. 12, in particular the value at $x = 1$ is equal to C_{PoSi}.

$$\begin{aligned} C_{eff}(x = 0) &= 8430 m/s \\ C_{eff}(x = 1) &= 3600 m/s \end{aligned} \tag{12}$$

This value of speed of sound is close to the one found in literature [9] even if the pore structure is not strictly identical.

4.3 Attenuation

Figure 9 shows the variation of the effective amplitude A_s as a function of the PoSi thickness. This curve is monotonous and decreasing and the attenuation for pure crystalline Silicon is very small, as expected. The observed error on this data can be caused by the angular position of the sample, which is not perfectly normal to the beam.

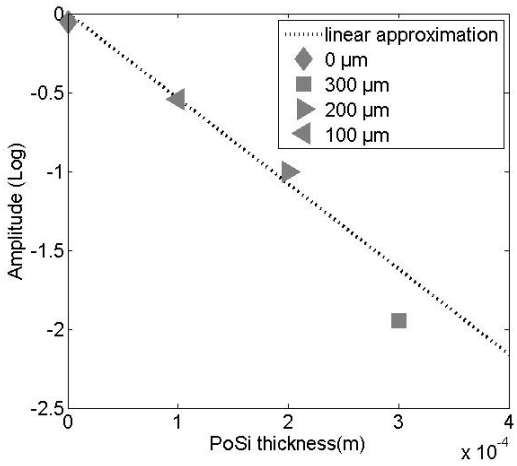

Figure 9: Attenuation in the PoSi layer a as function of its thickness.

An exponential fitting, as shown in figure 9, allows the attenuation coefficient to be measured (Eq. 13).

$$\alpha_{PoSi} \approx 5000\ Np/m \text{ at } 20MHz \tag{13}$$

5 Conclusion

In this study, measurements of attenuation and speed of sound have been performed in crystalline silicon wafers and in samples with different thicknesses of porous silicon layers (100, 200, 300 μm) using an insertion/substitution method. The amplitude of transmitted signals decreases with the porous layer thickness. This amplitude is divided by approximately 5 in the sample with a 300 μm thickness porous layer as compared to bulk silicon. The speed of sound also decreases with the porous layer thickness: the evolution can be explained by a simple linear model. This variation is also quite significant. In both cases, measured ultrasonic parameters can be used to characterize the PoSi layers. In particular, the measurement of these parameters can be a good indicator of the electrochemical etching depth. New measurements will be performed using two higher frequency transducers in order to separate the echoes in transmitted signals and estimate the attenuation and the phase velocity versus frequency in the transducer bandwidth. A sensitivity study will also be performed on many different porous layer thicknesses in order to estimate the precision of these measurements. Finally this study will be completed by measurements on samples with other porosity rates.

Acknowledgments

The authors thank the CERTEM.

References

[1] X. G. Zhang. Porous Silicon Formation and Electropolishing of Silicon by Anodic Polarization in HF Solution. *Journal of The Electrochemical Society*, 136(5):1561, 1989.

[2] H. Föll, M. Christophersen, J. Carstensen, and G. Hasse. Formation and application of porous silicon. *Materials Science and Engineering: R: Reports*, 39(4):93–141, November 2002.

[3] K. S. W. Sing. Reporting physisorption data for gas/solid systems with special reference to the determination of surface area and porosity (Recommendations 1984). *Pure and Applied Chemistry*, 57(4):603–619, 1985.

[4] HS Kim, DW Zheng, AJ Becker, and YH Xie. Spiral inductors on si p/p(+) substrates with resonant frequency of 20 GHz. *IEEE ELECTRON DEVICE LETTERS*, 22(6):275–277, 2001.

[5] C. Populaire, B. Remaki, M. Armenean, E. Perrin, O. Beuf, H. Saint-Jalmes, and D. Barbier. Integrated RF micro-coils on porous silicon. In *Proceedings of IEEE Sensors, 2004.*, pages 1064–1066. IEEE, 2004.

[6] S OZDEMIR and J GOLE. The potential of porous silicon gas sensors. *Current Opinion in Solid State and Materials Science*, 11(5-6):92–100, October 2007.

[7] V Lehmann, R Stengl, and A Luigart. On the morphology and the electrochemical formation mechanism of mesoporous silicon. *Materials Science and Engineering: B*, 69-70:11–22, January 2000.

[8] M Guendouz, P Joubert, and M Sarret. Effect of crystallographic directions on porous silicon formation on patterned substrates. *Materials Science and Engineering: B*, 69-70:43–47, January 2000.

[9] Raul José Da Silva Camara Mauricio Da Fonseca and J. Attal. Microcaractérisation élastique de matériaux poreux par signature acoustique = Elastic microcharacterization of porous materials by acoustic signature, 1995.

[10] P. A. Deymier, A. Khelif, B. Djafari-Rouhani, J. O. Vasseur, and S. Raghavan. Theoretical calculation of the acoustic force on a patterned silicon wafer during megasonic cleaning. *Journal of Applied Physics*, 88(5):2423, 2000.

[11] Wayne D. Wilson. Speed of sound in distilled water as a function of temperature and pressure. *The Journal of the Acoustical Society of America*, 31(8):1067–1072, 1959.

[12] H. J. McSkimin. A Water Immersion Technique for Measuring Attenuation and Phase Velocity of Longitudinal Waves in Plastics. *The Journal of the Acoustical Society of America*, 49(3B):713, 1971.

[13] J L Davis. *Wave propagation in solids and fluids*. Wave propagation in electromagnetic media. Springer-Verlag, 1988.

[14] D Royer and E Dieulesaint. *Elastic Waves in Solids: Free and guided propagation*. Advanced texts in physics. Springer, 2000.